Field-emission durability employing highly crystalline single-walled carbon nanotubes in a low vacuum with activated gas

Field-emission durability employing highly crystalline single-walled carbon nanotubes in a low vacuum with activated gas

Norihiro Shimoi [a)] and Kazuyuki Tohji

Graduate School of Environmental Studies, Tohoku University,
6-6-20 Aoba, Aramaki, Aoba-ku, Sendai 980-8579, Japan

[a)]Author to whom correspondence should be addressed:
Tel. & Fax.: +81-22-795-4584. E-mail: norihiro.shimoi.c8@tohoku.ac.jp

Abstract

A new approach to improving power consumption and energy efficiency is to use a simple structure with highly crystalline single-walled carbon nanotubes (hc-SWCNTs) in the cathode. We succeeded in determining the efficacy and applicability of the field emission (FE) properties of hc-SWCNTs in a low vacuum below 0.1 Pa with activated gas. In particular, the FE of 1.0 mA/cm^2 of hc-SWCNTs heated at 50 ℃ exhibits good stability for over 600 s in a low-vacuum atmosphere with oxygen added in a cathodic planar field emitter. The improved FE electrical properties of the hc-SWCNTs can likely be attributed to the increase in the crystallinity of the SWCNTs despite the low-vacuum atmosphere. It is further expected that the hc-SWCNT field emitters will be applicable to dry etching processes because single ionized molecules or radicals can be selectively synthesized with almost no energy loss and without requiring a cooling system. Our novel SWCNTs, as a component of a flat plane-emission device, may provide a technological breakthrough for realizing both energy saving and a low carbon

environment in dry etching processes as well as in semiconductor industrial development.

Introduction

Alternative technologies and approaches to save energy through low power consumption in our day to day activities have been extensively studied for semiconductor processes. Such efforts significantly contribute to achieving our goal of energy efficiency and sustainable energy through plasma processing in the semiconductor industry. For example, the developed electromagnetic processes, represented by plasma etching, are now widely used for etching in manufacturing semiconductors and other industrial scenes. However, the majority of plasma etchant equipment consumes much energy to sustain the high voltage and current load necessary to generate etchant radical ions. Instead of plasma etching processes, we focused on the development of a radical-ion-selective etchant by electron beam irradiation at a low energy from a cathode ray electrode and attempted to use highly crystalline carbon nanotubes (CNTs) as electron emitters. In particular, highly crystalline CNT field emitters in a vacuum atmosphere are expected to play a role in selectively producing a radical or ion in etching equipment, because of the narrow energy distribution of field emission (FE) electrons with high-current-density output and low acceleration energy.

Since the possibility of inventing electrical devices using CNTs was first predicted in a landmark paper by Rinzler et al. [1], carbon materials with one-dimensional shapes—such as CNTs and carbon nanofibers (CNFs)—have gained attention for their

use in electronic devices. Ideal crystalline single-walled carbon nanotubes (SWCNTs) possess unique physicochemical properties, including high chemical stability, thermal conductivity, mechanical strength, and electrical conductivity. They can be fabricated to be either metallic or semiconducting by controlling the way in which graphene is rolled up into a tube (i.e., diameter or chiral angle). This controllability is effective for developing electronic devices [2–5]. SWCNTs, which exhibit one-dimensional confinement effects, can be used as coherent quantum wires [6–8]. Also, SWCNTs with excellent mechanical properties [9] have been used over a wide range of applications including field emitters [1, 10–12], and they have been studied across a broad array of fields of applied research. However, they were inapplicable as electron sources with high stability and long durability because of their low electron emission efficiency with low loading power and short life of emitted radiation. One inherent obstacle has been that synthesized SWCNTs have crystal defects in their carbon network, which leads to unstable physicochemical properties, rendering their use problematic in electronic devices requiring high reliability. Many researchers have used untreated or only purified SWCNTs, mainly those grown by chemical vapor deposition, as it has been very difficult to handle CNTs manually. The control of their crystallinity and purity to obtain good stability and long durability has also been left unexamined, meaning that the crystallinity for a perfect carbon network has yet to be attained. Tohji et al. succeeded in purifying SWCNTs synthesized by arc discharge [13]. In addition, they succeeded in obtaining pure and highly crystalline SWCNTs (hc-SWCNTs) by annealing them at a high temperature of 1473 K and a low pressure below 10^{-5} Pa [14, 15] and established a method of evaluating the crystallinity of SWCNTs by cryogenic thermal desorption spectroscopy and high-resolution transmission electron microscopy (TEM) [14]. On the

basis of these achievements, a process of synthesizing hc-SWCNTs has essentially been realized; however, a technique employing hc-SWCNTs as parts in an electrical device remains elusive.

The application of ideal hc-SWCNTs as field emitters for use in the dry etching process is industrially promising and approaching practicality since single ionized molecules or radicals can be selectively synthesized with almost no energy loss and without requiring a cooling system because FE electrons have a small energy width [16–17]. Currently, dry etching using plasma atmosphere in the semiconductor industry consumes much energy and loses redundant energy, because plasma excitation requires high power consumption and redundant ionized molecules and radicals of etchant gas are activated for plasma excitation, which has a wide energy distribution [18–20]. We have carried out basic research to develop FE devices using commercially available SWCNTs synthesized by arc discharge [21] and succeeded in employing SWCNT field emitters as the cathode of a planar lighting device for the first time ever [22]. Some reports were expressed to develop ionizer using CNTs as cathodic electron source in mass analyzer [23–24], however, there was no report for electrical source as field emitters having CNTs with high stability and durability of electron emission current in activated gas atmosphere. The authors succeeded to develop FE electron source using hc-SWCNTs with large current, high stability and long durability for field emission in fluorine-based gas and oxygen gas atmosphere not only inert gases in our study. Here, we report the successful use of a planar hc-SWCNT field emitter as a planar electron emission source in a low vacuum filled with activated gas at pressures above 0.1 Pa. This hc-SWCNT field emitter exhibited extremely high FE current output, long durability, and low FE electron energy.

Experimental section

Analytical-grade reagents were used in the experiments. SWCNTs synthesized by arc discharge were suitable for preparing hc-SWCNTs by an annealing process [14, 15]. We prepared SWCNTs with various crystallinities to examine the effect of crystallinity on their electrical stability and reliability. The main hc-SWCNTs, the subject of this research, were synthesized by our original process [25]. We also evaluated commercial SWCNTs from Hanwha Chemicals Co., Ltd., Korea, as the references for FE characteristics. For FE measurements, thin film samples comprising SWCNTs in an In_2O_3-SnO_2 (tin-doped indium oxide; ITO) matrix were prepared. Commercial SWCNTs were used as references. To fabricate thin films with an ITO matrix, a nonionic dispersant was added to facilitate the dispersion of the SWCNTs, in the ITO precursor solution. The dispersant was agitated to form an impact buffer to alleviate the large impact force of dispersion using a jet mill machine (Star Burst Mini, Sugino Machine, Japan) and a homogenizer comprising 99% butyl acetate, ethyl cellulose (EC) (Wako, abt. 49% ethoxy 100 cP) as a dispersant to prevent the reaggregation of SWCNTs, and 95% sodium linear alkyl benzenesulfonate (DBS; Wako Co., Ltd., Japan). The initial mixture included the ITO precursor as a conductive matrix, DBS, and EC at a ratio of 1:600:4. In this study, a tin-doped indium oxide (ITO; Kojundo-Kagaku Co., Ltd., Japan) precursor solution was used to physically separate the SWCNT aggregates into thin bundles of a small number of SWCNTs with an average diameter of approximately 20 nm.

Figure 1 shows TEM (Hitachi High-Technologies Corporation, Japan) images of the

hc-SWCNTs (Fig. 1(a)) and the commercial, merely purified SWCNTs (Fig. 1(b)). The commercial SWCNTs were prepared previously as a reference for comparison when determining the effect of crystallinity. hc-SWCNTs in bundles were clearly observed in the TEM image of each tube wall, and were denoted as straight lines (Fig. 1(a)). However, the commercial SWCNTs exhibited a wavy defective lattice in the TEM image (Fig. 1(b)).

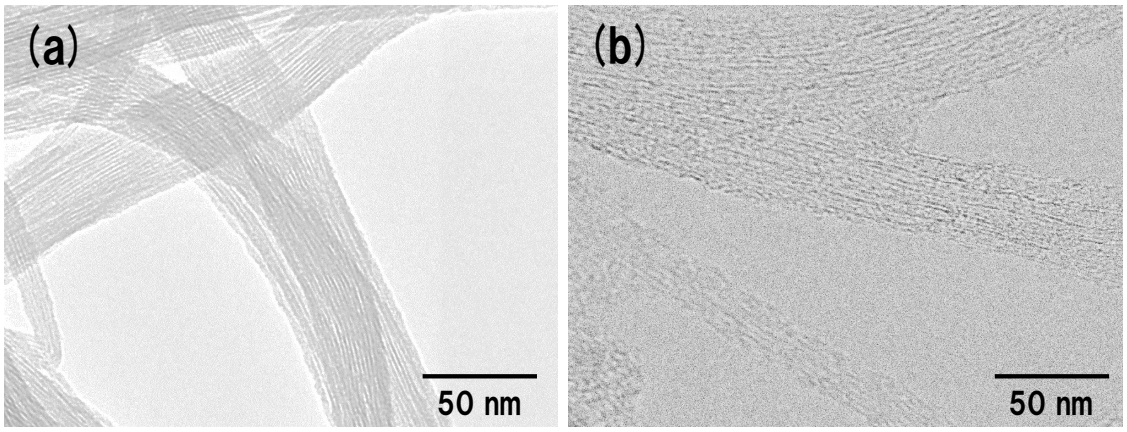

Fig. 1. TEM images with highly crystalline SWCNTs (a) and commercial SWCNTs as reference (b).

To verify the significance of employing SWCNTs in this work, several types of sample were prepared: SWCNTs in an ITO film, only an ITO film without SWCNTs, and SWCNTs on a graphite plate without ITO film. As a result, the samples without SWCNTs were confirmed to have no FE. To demonstrate the significance of employing hc-SWCNTs in electrical devices, the effect of increasing the crystallinity of SWCNTs on their electrical properties was examined by comparing hc-SWCNTs and unannealed SWCNTs with defects. The FE cathode with a weight density less than 1.0 mg/cm^2 was prepared by the electrostatic coating method, whereby the SWCNT mixture was stacked

on a grooved graphite plate, and then sintered at approximately 600 °C under 0.1 Pa. The FE cathode was then activated to induce FE by physically carving the coated film to expose the SWCNTs as field emitters, as shown in Fig. 2. The width of each nick in the FE cathode was 50 μm, and the film was patterned with straight nicks separated by an interval of 100 μm. Moreover, the ITO-mixed hc-SWCNT-coated film was patterned on top of a convex portion of a graphite plate with a distance of 20 μm between the neighboring nicks.

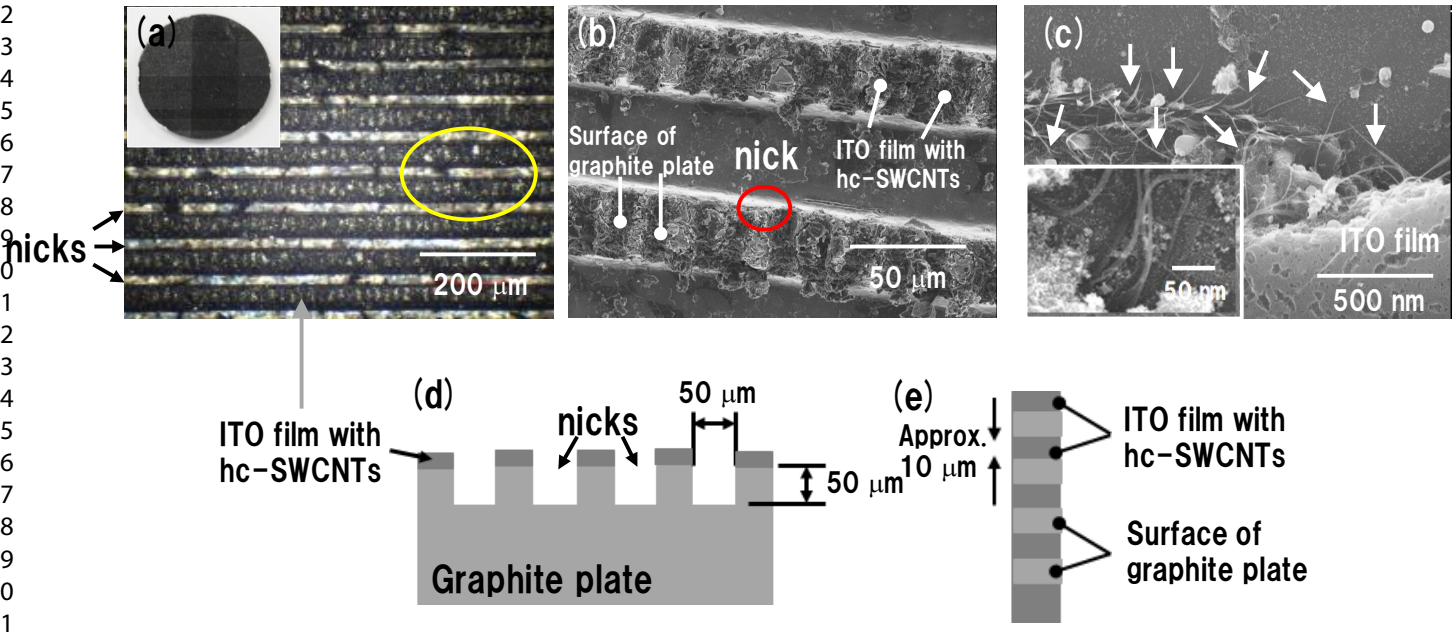

Fig. 2. Images of the FE electrode with hc-SWCNTs on a nicked graphite plate. (a) The inset shows the nicked surface of a graphite plate and a cathode electrode. (b) SEM image of the area in the yellow circle in (a). (c) SEM image of hc-SWCNTs exposed from the wall of the ITO film indicated by the red circle in (b), and the inset showed hc-SWCNT bundles enlarged the SEM image of (c). (d) Schematic of the cross-sectional view of FE cathode having a scratched graphite plate and ITO film with hc-SWCNTs. (e) Detailed schematic view of the top of a convex portion of a graphite plate.

The FE current measurement system is shown in Fig. 3. Once the cathode substrate including the SWCNTs was set onto an ITO-sputtered pattern on a glass substrate, the FE characteristics of the cathode were analyzed in a chamber. The thin-film coating with SWCNTs as the cathode was measured. Analyses included electron FE current density–electrical field (J–E) curves and their light emission homogeneity. The anode plate used to measure J–E curves and the homogeneity of planar emission was assembled by placing a green phosphor (ZnS:Cu,Al; Nichia Chemicals Co., Ltd., Japan) having a thickness of approximately 20 μm on the sputtered ITO film. The distance between the cathode surface and the anode electrode was controlled to be within 120 to 400 μm, and the gap was maintained constant using insulator spacers. The size of each measured FE emitter was 0.7×0.7 cm^2.

The sample was placed in a vacuum chamber at a low vacuum of less than 0.1 Pa and connected to an electrical circuit to measure the FE properties. The chamber had a gas insert line and a gauge to monitor the vacuum. The degree of vacuum in a chamber maintaining a gas at approximately 1 Pa was controlled by adjusting the gas injection pressure and the main valve for differential pumping. The FE measurement system shown in Fig. 3 was constructed from a power supply unit comprising an amplifier (Model 2210-CE; Trek Holding Co., Ltd., USA), a function generator (DF1906; NF Corporation, Japan), an oscilloscope to monitor FE current, and a PC to store the measured FE data. The voltage applied to the sample for FE measurements was designed to be a periodic rectangular wave with a frequency of 1 Hz and a duty of 20%. The FE current was measured as voltage data then converted using a resistor of 100 kΩ to 1 MΩ to prevent any signal noise during the measurement from being detected. In this study, oxygen as the oxidation gas, argon as the carrier gas, and sulfur hexafluoride

as the fluorine-based gas were used in the chamber, and the sample for measurements was set in the chamber to determine its J–E characteristics and FE durability.

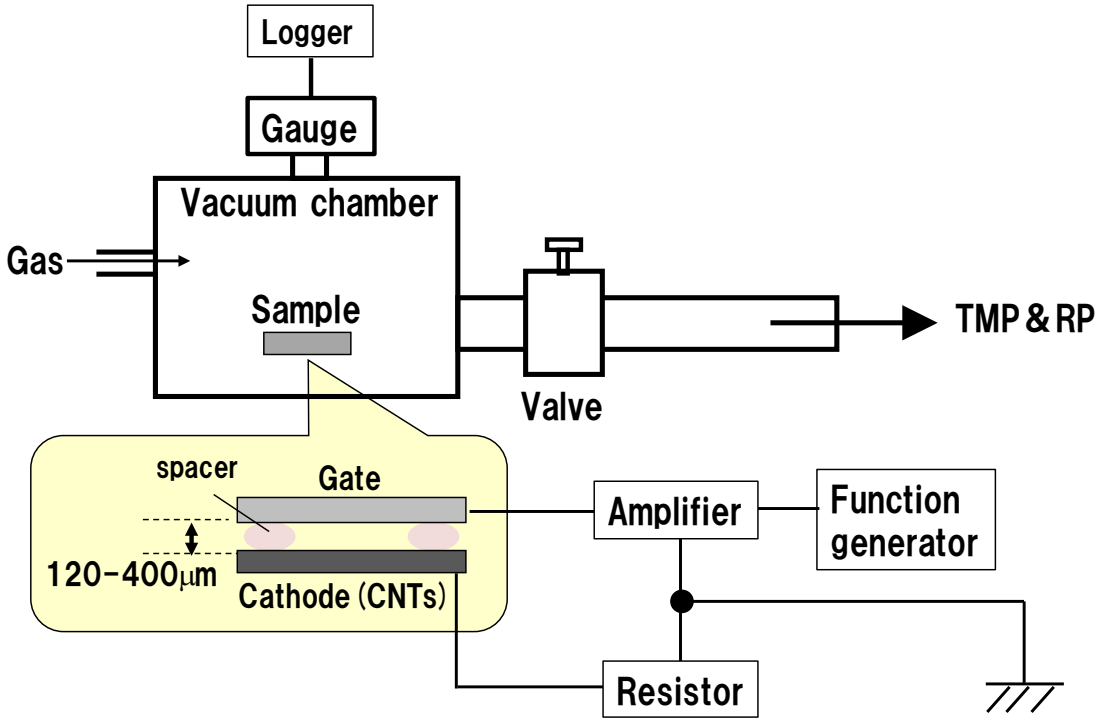

Fig. 3. Schematic of the FE sample and the details of the sample and electric circuit for FE measurement.

Results and Discussion

Field emission properties

Figure 4 shows the relationship between the FE current density and the electric field in a high vacuum of 4.0×10^{-3} Pa and a low vacuum of 2 Pa filled with argon (Ar) gas on a logarithmic scale (called the Fowler–Nordheim plot [26–32]) and planar lighting images. Overall, the turn-on fields for thin films with hc-SWCNTs and

commercial SWCNTs in a high vacuum of 4.0×10^{-3} Pa were less than 4 V/μm at 0.1 mA/cm^2. As shown in Figs. 4(a), (b), and (d), the J–E curves and the homogeneity of brightness spots in the films were similar among samples regardless of the SWCNT crystallization, indicating homogeneous probability densities of SWCNTs that induce FE in each sample.

Measurements were performed in a medium vacuum of 2 Pa argon gas after FE loading for 1 min. The FE curves and homogeneity of planar lighting spots of each SWCNT shown in Figs. 4(a), (c), and (e) were different from those of the hc-SWCNTs and commercial SWCNTs with crystal defects. Moreover, the mechanism of FE from each SWCNT and the atmosphere around the FE samples has been reported to follow the F–N tunneling model. The density of the electric potential concentrated at the tips of CNTs is decreased to a certain extent depending on their length and diameter, and the distance between neighboring CNTs. Electrons tunnel to the outside through the area with a thin quantum energy barrier localized near the tips of CNTs [33–37]. Table 1 summarizes the FE properties of each sample determined from the J–E curves in the cases of high vacuum and low vacuum with argon in Fig. 4(a). From the F–N plots in the inset of Fig. 4(a) converted to the applied field E – FE current density J characteristics obtained from FE measurements in Fig. 4(a), a significant difference was found between the total FE emission site area α and the field enhancement factor β, which is the ratio of the intensity of the electric field concentrated at the tips of the SWCNTs to the actual electric field, before and after FE loading in argon gas atmosphere. An average field factor β of approximately 1.8×10^6 cm^{-1} is estimated from the slope of the FN plot, in case that the work function for graphite is 4.8 eV. As a conservative estimate, $\beta \sim r^{-1}$ [38]. Therefore, a CNT tip radius of 5.7 nm is estimated

from the FN plot, which is in good agreement with the 7-nm tip radius estimate from SEM in Fig. 2(c). Such a difference was presumed to depend on the crystallinity of the SWCNTs. We infer that the hc-SWCNTs in a coated film will have good durability of FE properties in argon carrier gas during the dry etching process, although the FE properties of the commercial SWCNTs with crystal defects are degraded upon exposure to insert gases.

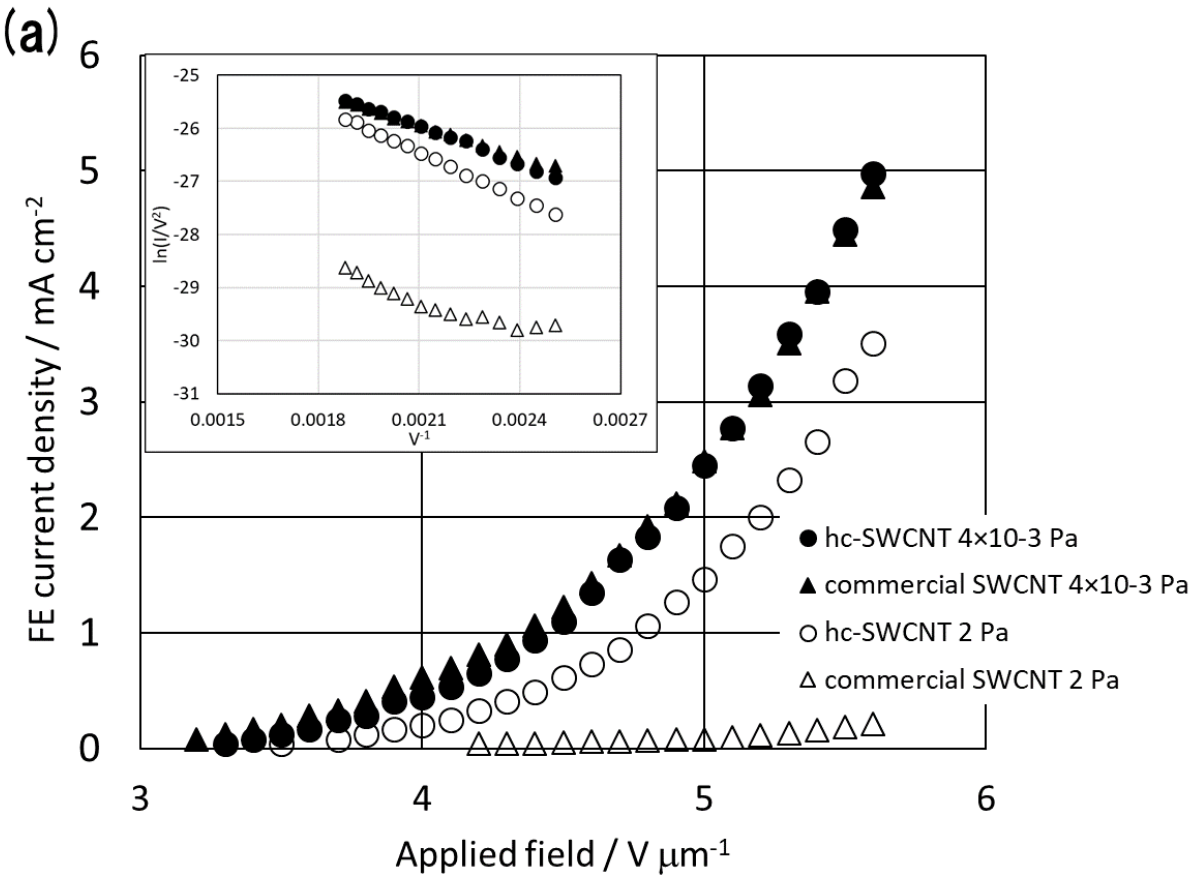

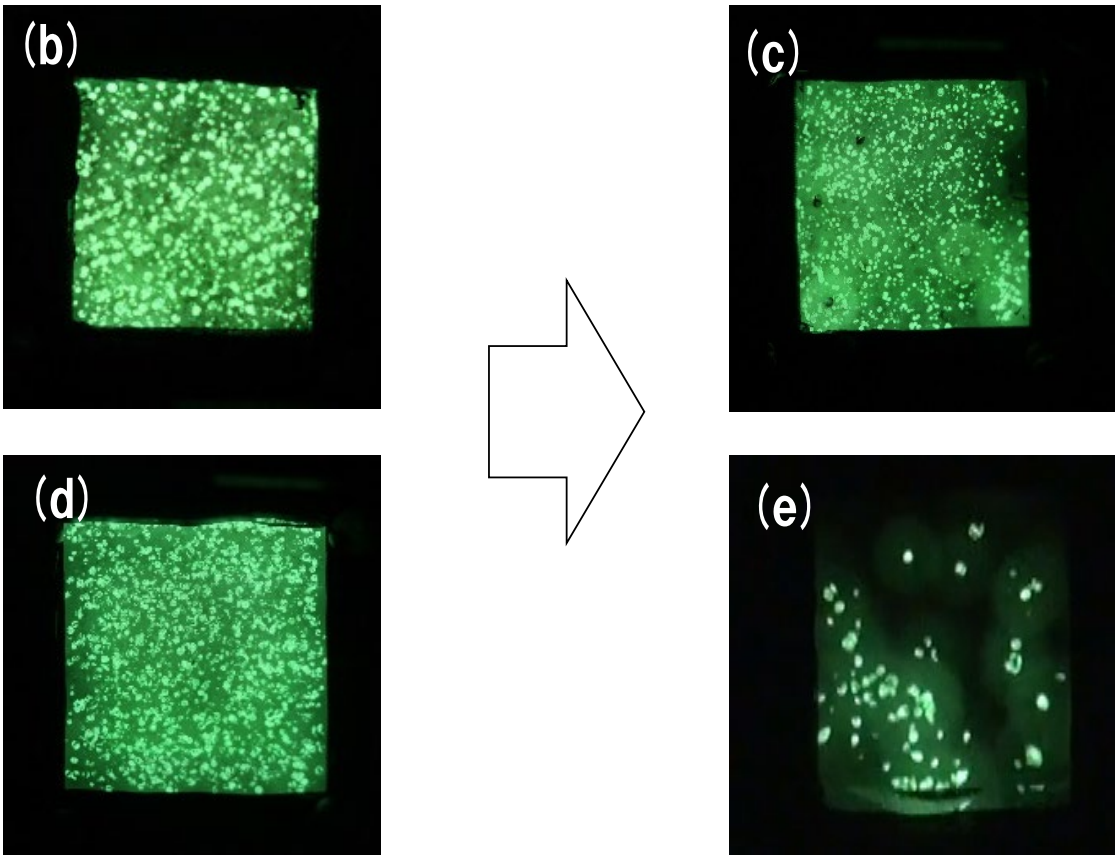

Fig. 4. Field-emission properties. (a) J–E curves with the inset of F–N plots. (b) and (c) Planar lighting images of films with hc-SWCNTs obtained using a neutral-density filter, (b) in a high vacuum of 10^{-3} Pa and (c) in a medium vacuum of 2 Pa argon gas atmosphere and FE current density of 2.5 mA/cm^2. (d) and (e) Planar lighting images of films with commercial SWCNTs (d) in a high vacuum of 10^{-3} Pa and (e) in a medium vacuum of 2 Pa argon gas atmosphere and FE current density of 2.5 mA/cm^2 obtained using a neutral-density filter.

Table 1. FE properties under various conditions.

Ar pressure (Pa)	hc-SWCNT		Commercial SWCNT	
	α (m^2)	β (cm^{-1})	α (m^2)	β (cm^{-1})
Approx. 4×10^{-3}	3.25×10^{-15}	1.77×10^{6}	1.55×10^{-15}	2.28×10^{6}
Approx. 2.0	1.55×10^{-15}	1.65×10^{6}	4.79×10^{-18}	1.42×10^{6}

Durability of hc-SWCNT loading field electron emission

Figure 5 shows FE lifetimes of the hc-SWCNTs with a supplied DC voltage of 500 V and a distance of 120 μm between the cathode and the gate in a vacuum of 1.2 Pa argon gas and a DC voltage of 1600 V and a distance of 400 μm between the cathode and the gate in a vacuum of 0.9 Pa argon gas. These cathodes, assembled in a simple diode structure with conductive anodes, were set at an initial FE current density of 1 mA/cm^2. The FE current density of the sample supplied with 1600 V in a vacuum of 0.9 Pa degraded markedly, and the FE current durability of the sample supplied with 500 V in a vacuum of 1.2 Pa was maintained for 600 s. The durability of the DC loading field emission current of each of the SWCNTs used as field emitters depends on the supplied voltage. The acceleration test is one way of supplying constant DC voltages to FE devices. With the application of a low voltage instead of a lower vacuum, hc-SWCNT devices again exhibit long durability of FE.

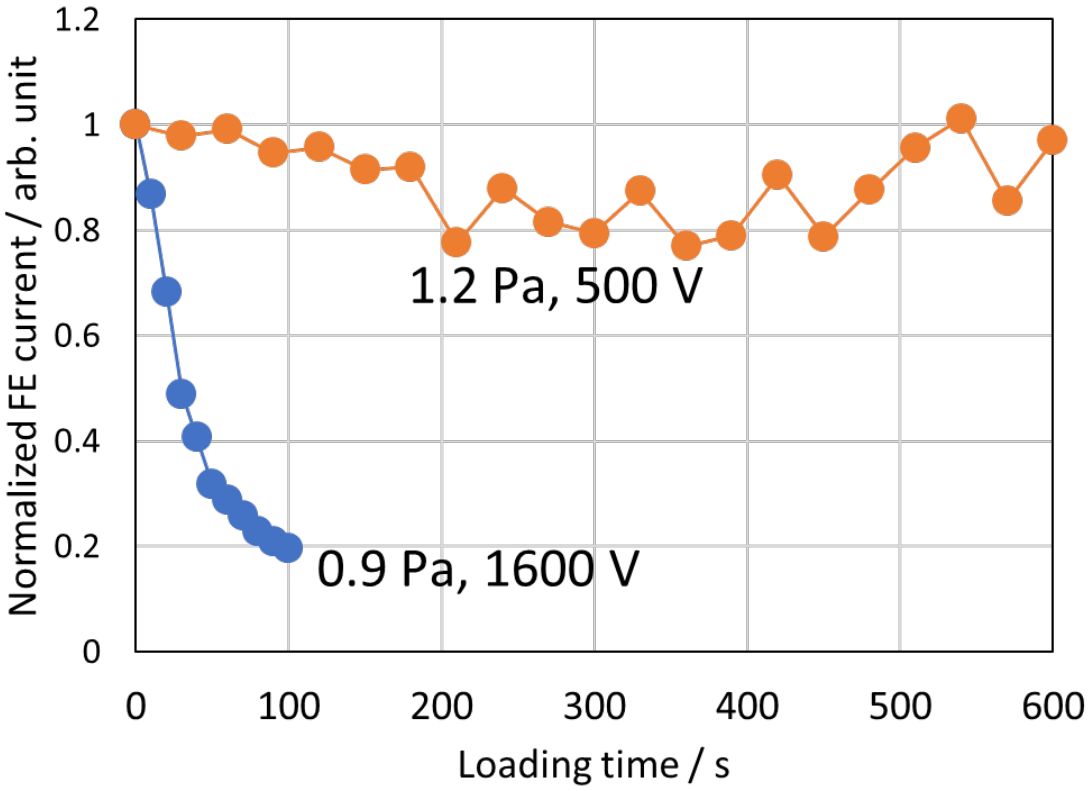

Fig. 5. FE durabilities at high and low loading voltages in argon gas atmosphere of low vacuum.

The SEM image in Fig. 6(a) shows hc-SWCNTs with an ITO matrix after the measurement of FE durability supplied with 1600 V in a vacuum of 0.9 Pa argon gas. The white dotted circle in Fig. 6(a) indicates SWCNT bundles with adhering indium compounds from the ITO matrix. The amount of indium contaminant around the hc-SWCNT bundles was measured from the TEM image in Fig. 6(b) and the atomic content ratio distribution of carbon and indium in Fig. 6(d) analyzed by energy-dispersive X-ray spectrometry (EDX; Hitachi High-Technologies Co., Ltd., Japan) along the white dashed line in Fig. 6(b). In addition, the TEM image in Fig. 6(c) shows a bared hc-SWCNT bundle without indium compounds contamination from the

sample after long-time measurement.

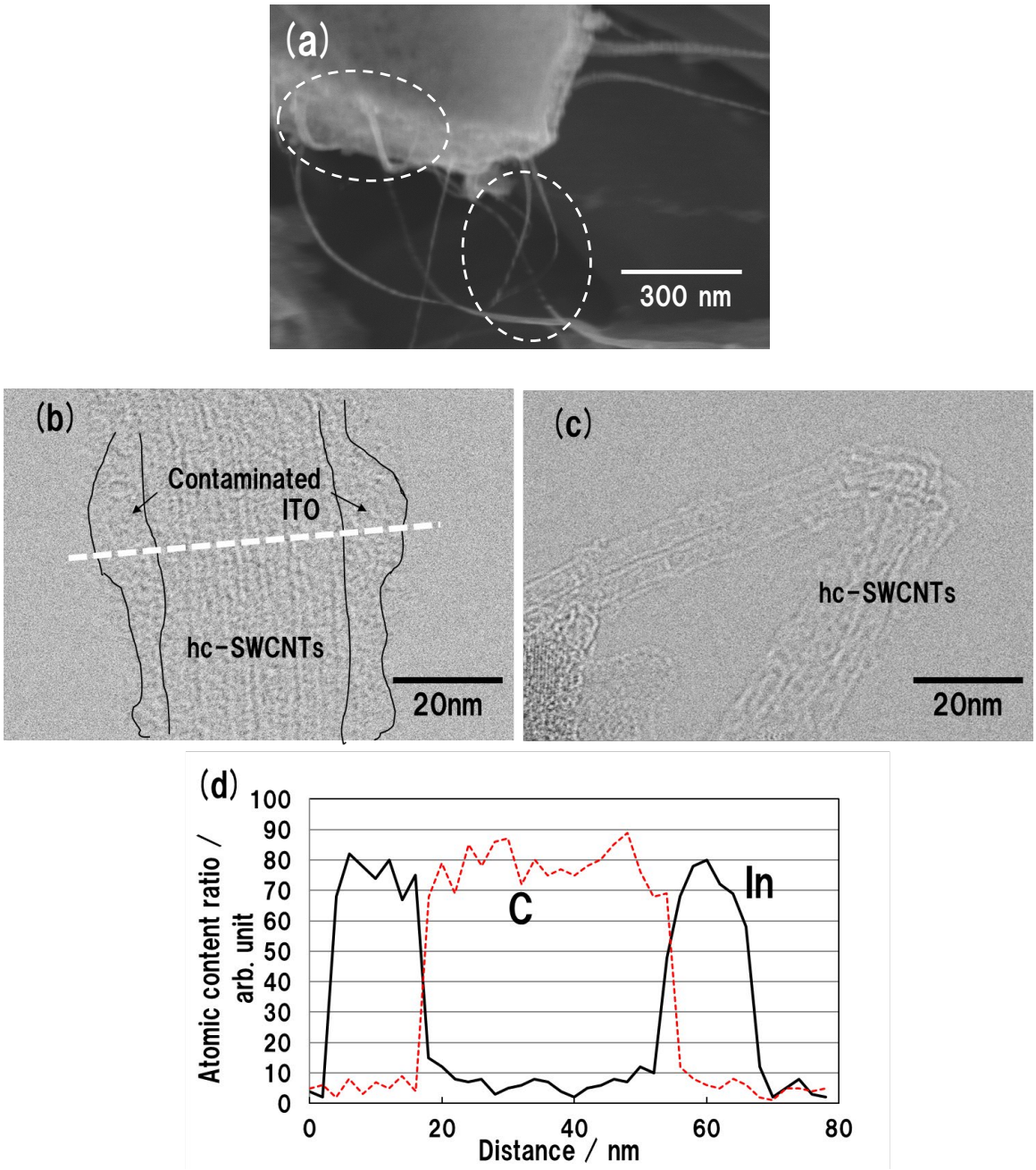

Fig. 6. SEM (a) and TEM ((b), (c)) images, and atomic content ratio distributions (d) of carbon (C) and indium (In) compounds on the surface of FE emitters with hc-SWCNTs in an ITO matrix. The SEM image (a) was taken after long-time measurement of FE emission durability with 1600 V applied in a vacuum of 0.9

Pa argon gas. The TEM images show the surface of hc-SWCNT bundles (b) with indium contamination after long-time measurement and (c) without indium compound contamination in the sample shown in SEM image (a). The hc-SWCNTs in image (b) were contaminated with indium compound material, as judged from the result of the atomic content ratio (d) of carbon and indium along the white dashed line in TEM image (b).

Figure 6 shows the FE lifetime of 600 s for hc-SWCNTs in (a) argon carrier gas, (b) oxygen oxidation gas, and (c) fluorine-based gas sulfur hexafluoride. Each FE sample with hc-SWCNTs, which has almost the same FE properties as those in terms of the emission site α and field enhancement factor β in high vacuum shown in Table 1, in the diode structure was prepared with a gap of 120 μm between the cathode and the gate electrode in each gas. To these cathode electrodes, a voltage of 500 V with a square pulse of duty 20% at a frequency of 1 Hz was applied, and an initial FE current of 1 mA/cm^2 was obtained in a vacuum atmosphere of less than 10^{-3} Pa. A heater ribbon for degassing the chamber was set around the outside of the chamber, and it was controlled to heat, but not anneal or bake, the FE emitter sample loaded into the chamber for FE measurement at 50 ℃. Each graph in Fig. 6 indicates the FE durability results obtained (i) in a low vacuum of approximately 1 Pa without heating the sample, (ii) in a high vacuum of approximately 10^{-3} Pa with heating of the sample after measurement (i) at 50 ℃, and (iii) in a low vacuum again with heating of the sample after measurement (ii). The FE current shown by (i) unheated hc-SWCNTs in low vacuum of each gas in the chamber, decreased markedly, and the FE current density with a heated sample in a high vacuum of approximately 10^{-3} Pa increased to approximately 1.0 mA/cm^2. The cause of this was assumed to be the cleaning of the SWCNT surfaces, which came into contact with light ions or radicals synthesized from the gas irradiated by FE electrons. This

cleaning would make it easy for electrons to be emitted from the tips of the SWCNTs. This result implied that the current density of hc-SWCNTs did not attenuate beyond 600 s of continuous loading of power; otherwise, the long durability of FE from hc-SWCNTs in a low vacuum was presumed to depend on the warming condition for the FE emitter sample. The attenuation of the loading FE current depends on the crystallinity of each SWCNT in field emitters. The SWCNTs with high crystallinity showed superior performance characteristics for FE properties at a stable current density in a low vacuum with a low voltage of approximately 100 V.

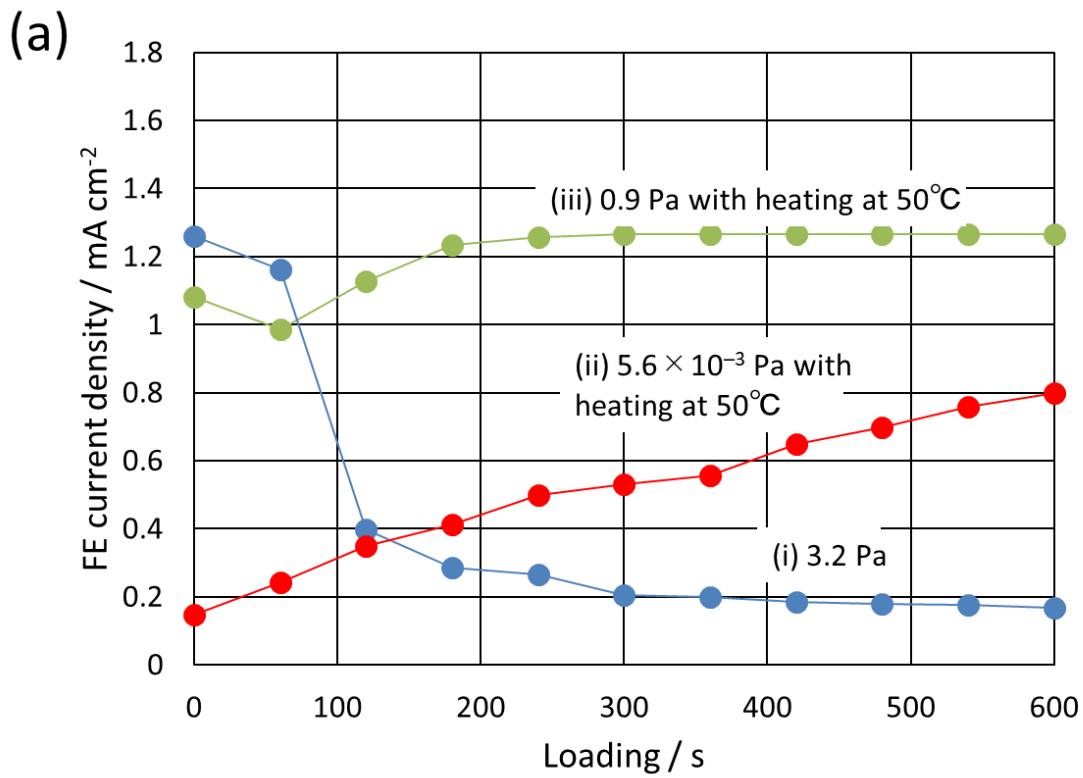

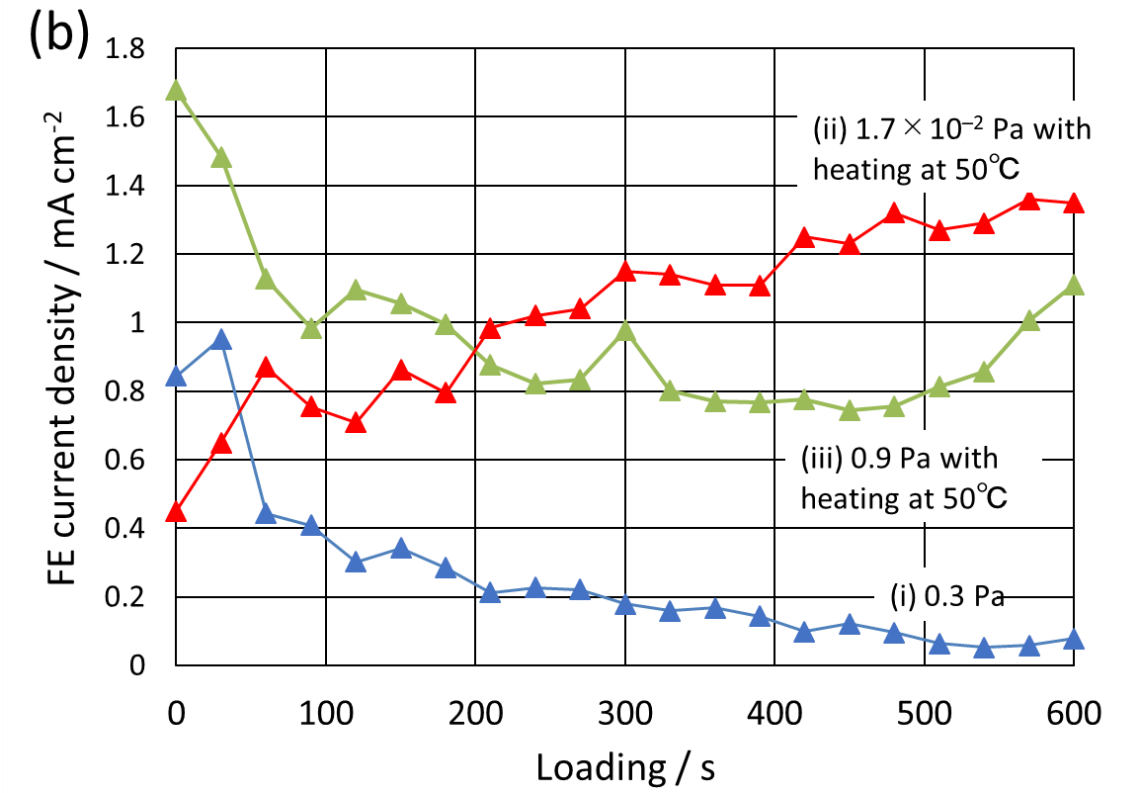
(b)
FE current density / mA cm-2
1.8
1.6
1.4
1.2
1
0.8
0.6
0.4
0.2
0
0
100
200
300
400
500
600
Loading / s
(ii) 1.7 × 10−2 Pa with heating at 50°C
(iii) 0.9 Pa with heating at 50°C
(i) 0.3 Pa

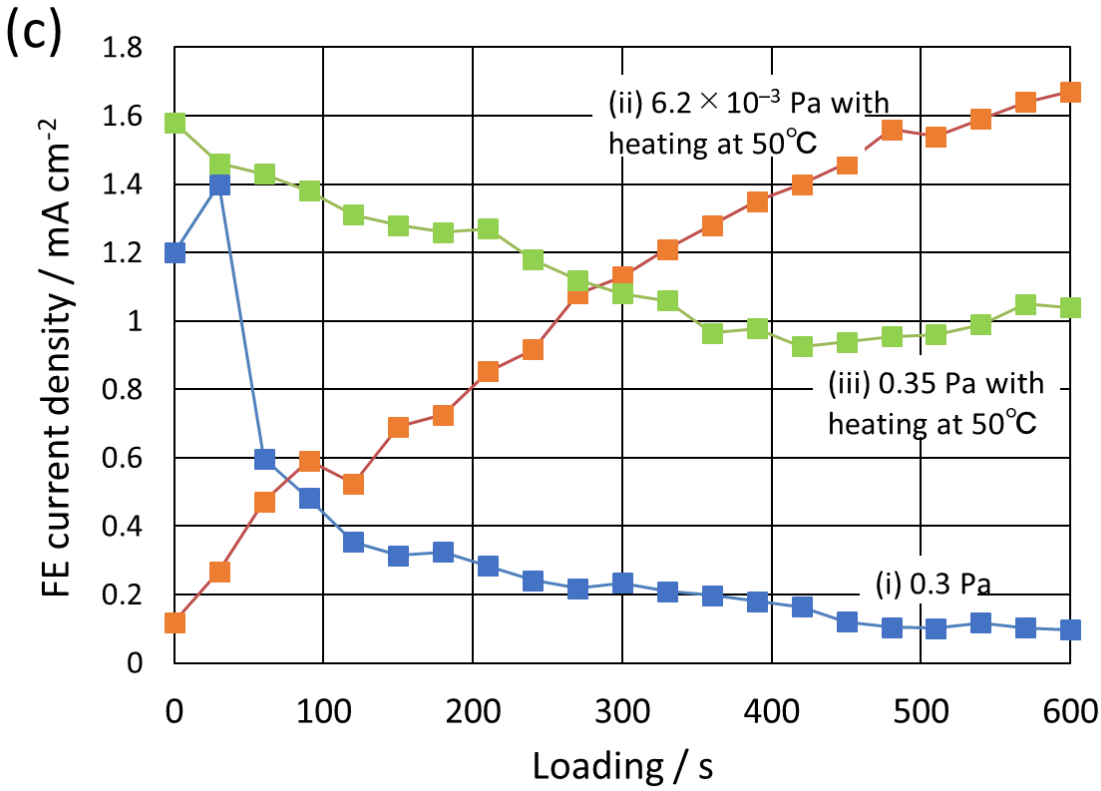
(c)
FE current density / mA cm-2
1.8
1.6
1.4
1.2
1
0.8
0.6
0.4
0.2
0
0
100
200
300
400
500
600
Loading / s
(ii) 6.2 × 10−3 Pa with heating at 50°C
(iii) 0.35 Pa with heating at 50°C
(i) 0.3 Pa

Fig. 7. Durability of FE current density up to 600 s of applying 500 V voltage with a square pulse duty of 20% at a frequency of 1 Hz. The radioactive half-life is defined as the time taken for the field emission current density to become half the initial value. (a) Ar atmosphere. (b) O_2 atmosphere. (c) SF_6 atmosphere.

We succeeded in obtaining good FE durability with a loading current density of 1 mA/cm^2, by employing hc-SWCNTs in a low vacuum with argon, oxygen, and sulfur hexafluoride. Figure 8 shows the results for each gas (argon, oxygen, and sulfur hexafluoride) at various partial pressures in the chamber before and after FE durability measurement using a quadrupole mass spectrometer (M-101QA-TDF; Canon Anelva Co., Ltd., Japan). We were able to ascertain the partial pressure of those light ions generated by FE electrons bombarding the argon, oxygen, and sulfur hexafluoride gases through FE durability measurement.

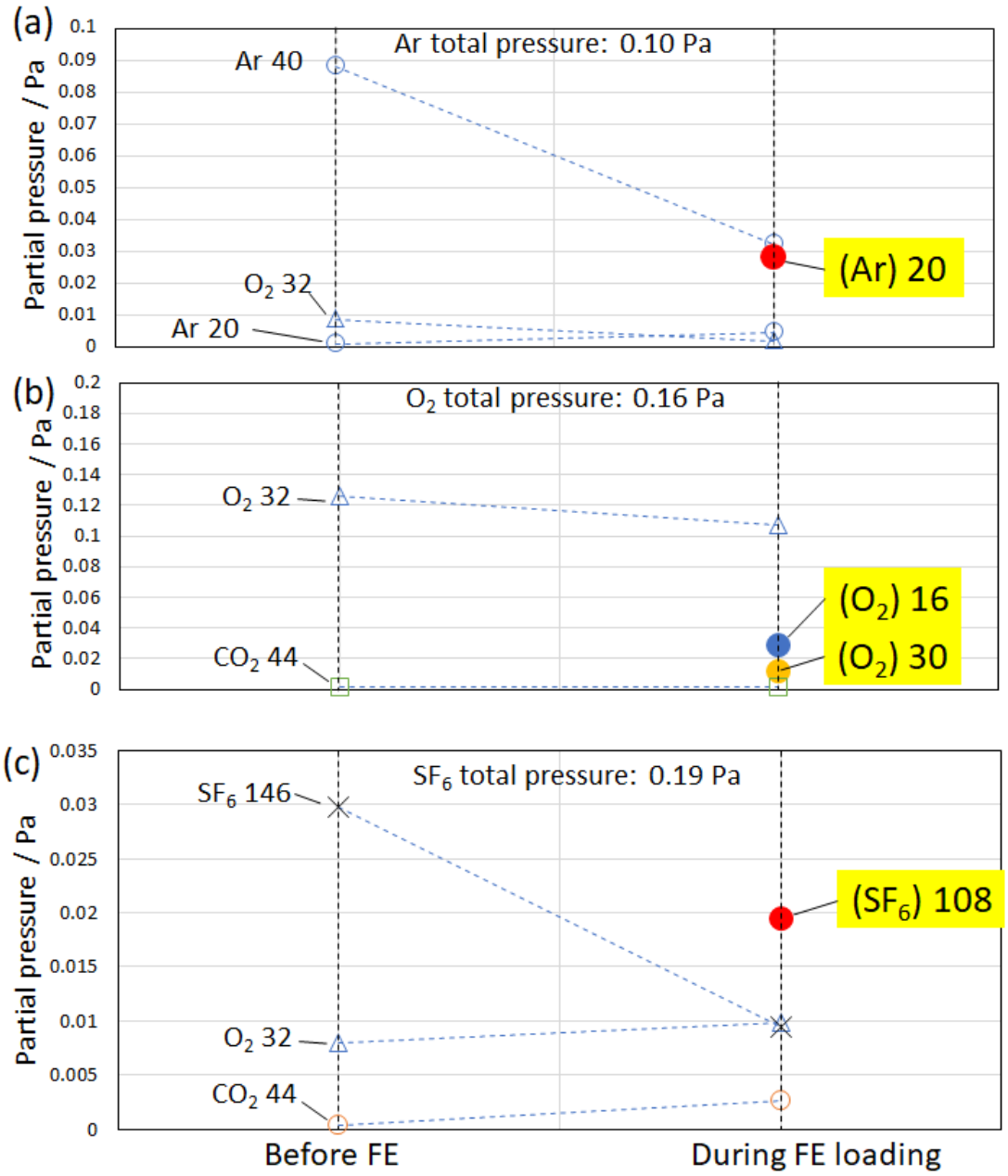

Fig. 8. Partial pressure of each gas (Ar, O_2, SF_6) in the chamber before and after FE loading. (a) Ar gas at a total chamber pressure of 0.10 Pa. (b) O_2 at a total chamber pressure of 0.26 Pa. (c) SF_6 at a total chamber pressure of 0.19 Pa. The FE loading current density was fixed at 1 mA/cm^2.

For reference, the SEM images in Fig. 9 show hc-SWCNTs with an ITO matrix after FE durability measurement in a low-vacuum atmosphere filled with a oxygen (O_2) and a sulfur hexafluoride (SF_6). The image for the case of argon gas has already been shown in Fig. 6. We observed some hc-SWCNTs bundles contaminated with indium compounds in Fig. 9. In particular, the surface morphology of SWCNTs in a low vacuum with O_2 gas after durability measurement was altered.

We inferred that the ionized or radical gas molecules were generated by the sputtering of FE electrons onto the ITO matrix with the SWCNTs. To obtain a stable current with high density, it is generally necessary to construct a triode structure vertically and uniformly positioned on an electrode by CVD at a high temperature in a high-vacuum atmosphere. Here, however, we obtained a stable current without the above-mentioned treatment and induced FE in a low vacuum in activated gas. The results in Figs. 6, 7, and 8, indicated that the high crystallinity of SWCNTs prevented the collapse of the carbon network upon the bombardment of ionized or radical molecules. Moreover, it was inferred that the attenuation of FE current of the FE cathode in a low vacuum with gas activated by low-energy FE electrons caused the degradation of the emission sites on the hc-SWCNTs as a result of the covering or adhesion of indium or indium compounds on the surface of hc-SWCNTs.

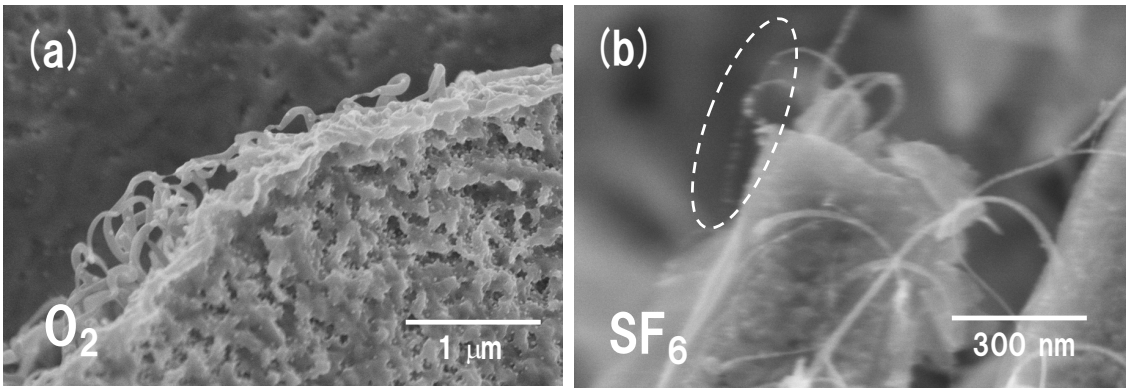

Fig. 9. SEM images of the surface of FE emitters with hc-SWCNTs after long-time measurement of FE emission durability in O_2 (a) and SF_6 (b) gases.

The above results indicated that the use of hc-SWCNTs realized durable FE with almost no marked attenuation in a low vacuum, and thus, these hc-SWCNTs can be used as field emitters in activated gas. We briefly explained of the effect of the increased crystallinity of SWCNTs synthesized by arc discharge on their FE properties. hc-SWCNTs hold promise for use as field emitters with stable FE.

Discussion

We successfully employed hc-SWCNTs as field emitters and obtained good FE durability in a low vacuum with gases; in particular, oxygen oxidation gas, argon carrier gas, and fluorine-based sulfur hexafluoride gas were used in this research. FE emitters are typically sensitive to bombardment of the ionized or dissociated gas on the emitted electrons; therefore, it has been thought to be important that FE emitters acting as cold cathodes were placed in a high-vacuum atmosphere to obtain a stable FE current. In this research, we found that hc-SWCNT FE emitters emit electrons in a low vacuum of 0.1−

10 Pa with activated gas.

Figure 10 shows the mechanism of ion or radical generation from the atmosphere gas by FE electron irradiation and its effects on SWCNTs. Electrons from FE emitters attack the argon, oxygen, or sulfur hexafluoride gas molecules surrounding FE emitters, and the gas molecules are activated to become ions or radicals. These ionized or radical molecules attack the SWCNTs, like reverse sputtering. The acceleration energy of the ionized or radical molecules depends on the energy of FE electrons attacking the gas molecules. When the energy of FE electrons is low, it is presumed that only the ITO matrix is attacked while hc-SWCNTs remain undamaged when hc-SWCNTs have been heated at 50 ℃, because the carbon network of SWCNTs shows no collapse even after this reverse sputtering. hc-SWCNTs are covered with sputtered indium compounds from the ITO matrix after the attack by the ionized molecules or radicals having a high energy of 1600 eV and the FE current with constant voltage is attenuated. On the other hand, in this research, when the ionized molecules or radicals attacked SWCNTs with crystal defects, they caused damage to the carbon networks of SWCNTs and FE attenuation. The above results showed that the FE stability of hc-SWCNTs as field emitters differs depending on the atmosphere gas; in particular, we found that hc-SWCNTs in an inert gas give a stable FE current in a low vacuum below 1 Pa.

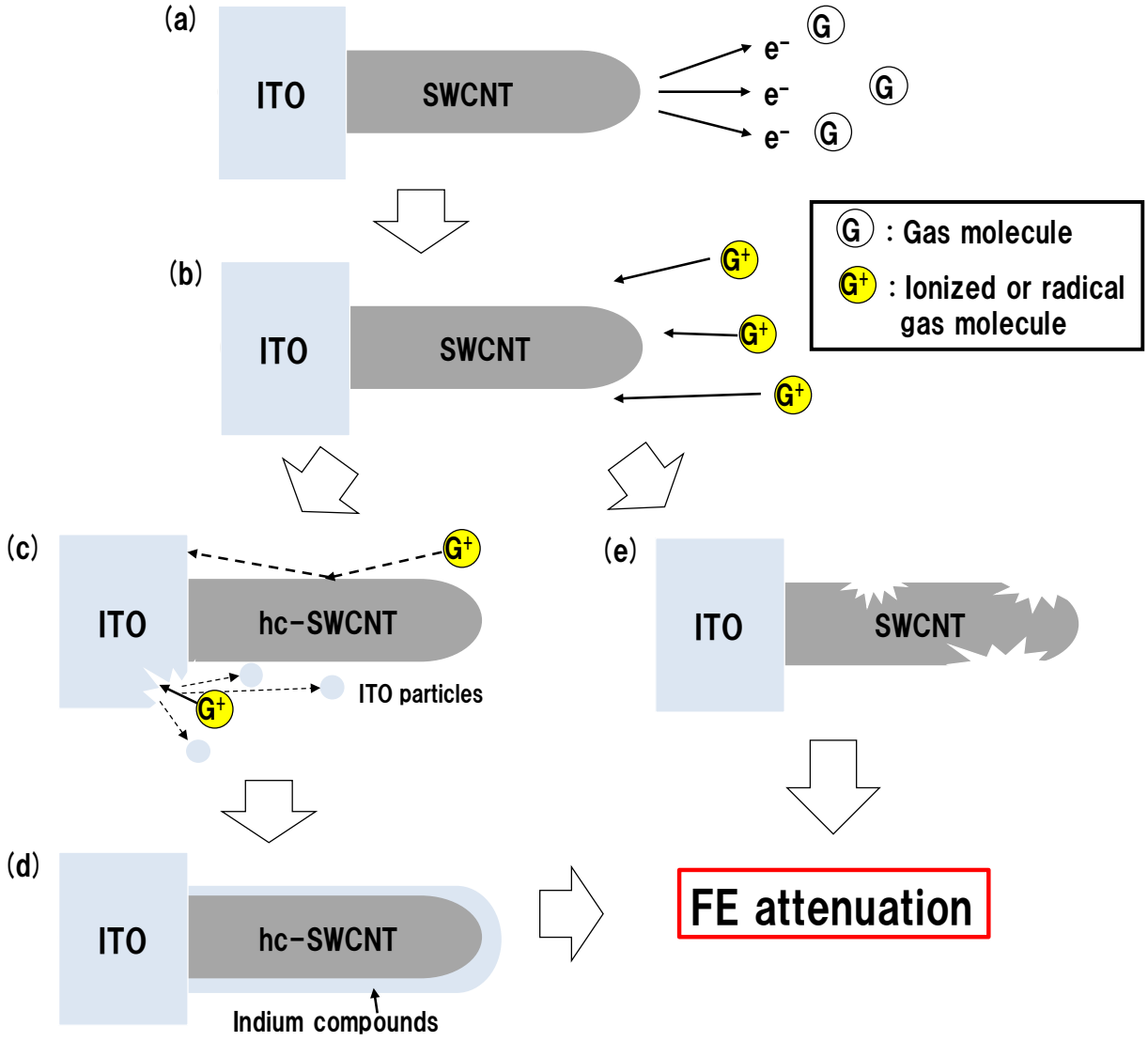

Fig. 10. Mechanism of FE attenuation.

(a) FE electrons attack Ar, O_2 or SF_6 molecules that become ionized or activated in radicals.

(b) The ionized or radical molecules activated by FE electrons bombard the electron-emitting SWCNTs.

(c) Low-energy ions or radicals do not damage hc-SWCNTs that have been heated at 50 ℃ and only sputter the ITO matrix.

(d) The hc-SWCNT is covered by indium compounds upon ion or radical bombardment, and the FE current is attenuated.

(e) When SWCNTs with crystal defects are used as FE emitters, the crystallinity of SWCNTs is degraded and the FE current is attenuated.

Conclusions

We applied original SWCNTs with high crystallization as the field emitters of planar electron emission devices. The high crystallinity of SWCNTs is one essential element in the fabrication of electronic devices with high stability and reliability for selectively obtaining ionized etchant molecules or radicals for the dry etching process. We believe that we have succeeded in realizing the homogeneous planar lighting of hc-SWCNTs for the first time ever [39]. The hc-SWCNTs are expected to significantly improve the FE properties compared with those of the devices fabricated with conventional materials. In particular, the hc-SWCNTs are expected to serve as field emitters that can emit electrons stably in a low vacuum below 1 Pa in an argon, oxygen, or sulfur hexafluoride gas atmosphere and realize high power output, a long lifetime of FE current, and the fabrication of a large-scale planar emission source.

The above-described discovery of the improved FE electrical properties of hc-SWCNTs are attributable to the increase in the crystallinity of the SWCNTs despite the low-vacuum atmosphere. A planar field emitter employing hc-SWCNTs will have high stability and high emission site homogeneity in activated gases, oxygen or fluorine compound gas; it will also have a long emission lifetime that will enable its practical use as an electron-emitting device for the selective generation of ionized molecules or radicals for dry etching in semiconductor processing.

Acknowledgements

The outcome of this study was derived through joint research conducted with Tokyo Electron Miyagi Ltd. (TEL). The authors would like to express their gratitude to TEL

for helpful discussions and proposals provided. Moreover, this study was conducted as a project consigned by the New Energy and Industrial Technology Development Organization and supported by JSPS KAKENHI Grant Number JP26220104. We would like to express our sincere gratitude for the guidance received.

References

1. A. G. Rinzler, J. H. Hafner, D. T. Colbert, and R. E. Smalley, "Field emission and growth of fullerene nanotubes," Mat. Res. Soc. Symp. Proc. **359**, 61 (1995).
2. N. Hamada, S. Sawada, and A. Oshiyama, "New one-dimensional conductors: Graphitic microtubules," Phys. Rev. Lett. **68**, 1579–1581 (1992).
3. J.-Y. Kim, M. Kim, H. M. Kim, J. Joo, and J.-H. Choi, "Electrical and optical studies of organic light emitting devices using SWCNTs-polymer nanocomposites," Opt. Mater. **21,** 147–151 (2002).
4. Y. Saito and S. Uemura, "Field emission from carbon nanotubes and its application to electron sources," Carbon **38**, 169–182 (2000).
5. G. Y. Liu, Q. N. Lv, S. H. Xia, D. A. Wang, T. X. Li, H. Y. Li, Y. G. Ding, and Z. M. Ju, "An improvement on cold carbon field-electron emitter for commercial X-ray tube," 2007 IEEE 20th International Vacuum Nanoelectronics Conference (2007) 63–64.
6. J. W. G. Wildoerm, L. C. Venema, A. G. Rinzler, R. E. Smalley, and C. Dekker, "Electronic structure of atomically resolved carbon nanotubes," Nature **391**, 59–62 (1998).
7. T. W. Odom, J. L. Huang, P. Kim, and C. M. Lieber, "Atomic structure and electronic properties of single-walled carbon nanotubes," Nature **391**, 62–64 (1998).

8. E. P. Sheshin, A. V. Anashchenko, and S. G. Kuzmenko, "Field emission characteristics research of some types of carbon fibres," Ultramicroscopy **79**, 109–114 (1999).
9. M. M. J. Treacy, T. W. Ebbesen, and J. M. Gibson, "Exceptionally high Young's modulus observed for individual carbon nanotubes," Nature **381**, 678–680 (1996).
10. Y. Saito, S. Uemura, and K. Hamaguchi, "Cathode ray tube lighting elements with carbon nanotube field emitters," Jpn. J. Appl. Phys. **37**, L346–348 (1998).
11. Y. Saito, "Carbon Nanotube and Related Field Emitters: Fundamentals and Applications," Weinheim, Germany, Wiley-VCH (2000).
12. P. R. Bandaru, "Electrical Properties and Applications of Carbon Nanotube Structures," J. Nanosci. Nanotechnol. **7**, 1239–1267 (2007).
13. K. Tohji, T. Goto, H. Takahashi, Y. Shinoda, N. Shimizu, B. Jeyadevan, I. Matsuoka, Y. Saito, A. Kasuya, T. Ohsuna, K. Hiraga, and Y. Nishina, "Purifying single-walled nanotubes." Nature **383**, 679 (1996).
14. S. Iwata, Y. Sato, K. Nakai, S. Ogura, T. Okano, M. Namura, A. Kasuya, K. Tohji, and K. Fukutani, "Novel method to evaluate the carbon network of single-walled carbon nanotubes by hydrogen physisorption," J. Phys. Chem. C Lett. **111**, 14937–14941 (2007).
15. N. Shimoi, Y. Sato, and K. Tohji, "Highly crystalline single-walled carbon nanotube field emitters: Energy-loss-free high current output and long durability with high power," ACS Appl. Electron. Mater. **1**(2), 163–171 (2019).
16. J.-M. Bonard, J.-P. Salvetat, T. Stöckli, L. Forr´o, and A. Châtelain, "Field emission from carbon nanotubes: perspectives for applications and clues to the emission mechanism," Appl. Phys. A **69**, 245–254 (1999).

17. K. Kimoto, "Practical aspects of monochromators developed for transmission electron microscopy," Microscopy **63**(5), 337–344 (2014).
18. H. Sugawara, Y. Ishihara, R. Saito, and Y. Sakai, Computational study on fundamental properties of CF_4/N_2 plasmas and application of impulse-field electron acceleration to CF_4 decomposition, *Proceedings of* the *XXVIIth ICPIG* p.18, Eindhoven, the Netherlands (2005).
19. K. E. Evdokimov, M. E. Konischev, V. F. Pichugin, and Z. Sun, "Study of argon ions density and electron temperature and density in magnetron plasma by optical emission spectroscopy and collisional-radiative model," Resource-Efficient Technologies **3**, 187–193 (2017).
20. Z. Chen, V. M. Donnelly, D. J. Economou, L. Chen, M. Funk, and R. Sundararajan, "Measurement of electron temperatures and electron energy distribution functions in dual frequency capacitively coupled CF_4/O_2 plasmas using trace rare gases optical emission spectroscopy," J. Vac. Sci. Technol. A **27**(5), 1159–1165 (2009).
21. N. Shimoi, L. E. Adriana, Y. Tanaka, and K. Tohji, "Properties of a field emission lighting plane employing highly crystalline single-walled carbon nanotubes fabricated by simple processes." Carbon **65**, 228–235 (2013).
22. S. B. Garrido, N. Shimoi, D. Abe, T. Hojo, Y. Tanaka, and K. Tohji, "Planar light source using a phosphor screen with single-walled carbon nanotubes as field emitters." Rev. Sci. Inst. **85**, 104704 (2014).
23. L. F. Velásquez-García, B. Gassend, and A. I. Akinwande, "CNT-based MEMS Ionizers for Portable Mass Spectrometry Applications," Journal of Microelectromechanical Systems **19**(3), 484–493 (2010).
24. C. A. Bower, K. H. Gilchrist, J. R. Piascik, B. R. Stoner, S. Natarajan, C. B. Parker,

S. D. Wolter, and J. T. Glass, "On-chip electron-impact ion source using carbon nanotube field emitters," Appl. Phys. Lett. **90**, 124102 (2007).

25. K. Yokoyama, S. Yokoyama, Y. Sato, K. Hirano, S. Hashiguchi, K. Motomiya, H. Ohta, H. Takahashi, K. Tohji, and Y. Sato, "Efficiency and long-term durability of nitrogen-doped single-walled carbon nanotube electrocatalyst synthesized by defluorination-assisted nanotube substitution for oxygen reduction reaction," J. Mater. Chem. A, **4**, 9184–9195 (2016).
26. Y. Gotoh, D. Nozaki, H. Tsuji, and J. Ishikawa, "Significant improvement of the emission property of Spindt-type platinum field emitters by operation in carbon monoxide ambient," Appl. Phys. Lett. **77**(4), 588–590 (2000).
27. C. A. Spindt, "A thin film field emission cathode," J. Appl. Phys. **39**, 3504–3505 (1968).
28. C. A. Spindt, I. Brodie, L. Humphrey, and E. R. Westerberg, "Physical properties of thin-film field emission cathodes with molybdenum cones, " J. Appl. Phys. **47**(12), 5248–5263 (1976).
29. G. Sanborn, S. Turano, P. Collins, and W. J. Ready, "A thin film triode type carbon nanotube field emission cathode," Appl. Phys. A, **110**, 99–104 (2012).
30. W. I. Milne, K. B. K. Teo, G. A. J. Amaratunga, P. Legagneux, L. Gangloff, J. P. Schnell, V. Semet, V. Thien Binh, and O. Groening, "Carbon nanotubes as field emission sources," J. Mater. Chem. **14**, 933–943 (2004).
31. L. H. Thuesen, "Effects of color phosphors on the lifetime of field emission carbon thin films," J. Vac. Sci. Tech. B, **19**, 3, 888–891 (2001).
32. V. S. Bormashov, K. N. Nikolski, A. S. Baturin, and E. P. Shesin, "Prediction of field emitter cathode lifetime based on measurement of I–V curves," Carbon **215**,

178–190 (2003).

33. R. Gomer, Field Emission and Field Ionization, Cambridge: Harvard University Press (1961).
34. R. Saito, M. Fujita, G. Dresselhaus, and M.S. Dresselhaus, "Electronic structure of chiral graphene tubules," Appl. Phys. Lett. **60**, 2204–2206 (1992).
35. K. Tanaka, K. Okahara, M. Okada, and T. Yamabe, "Electronic properties of bucky-tube model," Chem. Phys. Lett. **191**(5), 469–472 (1992).
36. N. Shimoi and K. Tohji, "Current-fluctuation mechanism of field emitters using metallic single-walled carbon nanotubes with high crystallinity," Appl. Sci. **7**(12), 1322 (2017).
37. B. R. Chalamala, R. M. Wallace, and B. E. Gnade, "Gas-induced current decay of molybdenum field emitter arrays," J. Vac. Sci. Technol. B, **17**, 303 (1999).
38. D. G. Pflug, "Modeling the effects of device scaling on field emitter array performance," M.S. thesis, MIT, Cambridge, MA (1996).
39. N. Shimoi, D. Abe, K. Matsumoto, Y. Sato, and K. Tohji, "Low-power-consumption flat-panel light-emitting device driven by field-emission electron source using high-crystalline single-walled carbon nanotube", Jpn. J. Appl. Phys. **56**, 07GE01 (2017).